DFT and Microkinetic Study of Acetylene Hydrogenation and Decomposition over the (111) surfaces of Pd, M and PdM alloys (M=Cu, Ag, Au)

Yugai Huang[1,2], Hui-Li Lu[1], Zhao-Xu Chen[1]*

[1] Institute of Theoretical and Computational Chemistry, Key Laboratory of Mesoscopic Chemistry of MOE, School of Chemistry and Chemical Engineering, Nanjing University, Nanjing 210023, China

[2] School of Life Sciences, Chemistry & Chemical Engineering, Jiangsu Second Normal University, Nanjing, China

Adsorption

1. CHCH

On Pd(111), acetylene preferentially adsorbs at the 3-fold hollow sites, with the adsorption energy of −2.02 eV, consistent with previous study[1]. On Ag(111) and Au(111), the adsorption energy of acetylene decreases to −0.04 eV on Ag(111) and −0.17 eV on Au(111). However, on Cu(111) surface it prefers to adsorb at the "4-fold diagonal hollow" site with an adsorption energy of −1.14 eV, which agrees with the experimental and theoretical results reported in literature[2,3]. When alloyed with Pd, the adsorption of acetylene on the three coin metal alloy surface increases, being −1.42eV on PdCu(111), −1.22eV on PdAg(111) and −1.14eV on PdAu(111). These values are close to the result on Cu(111). The decreasing order of adsorption energy from PdCu(111), PdAg(111) to PdAu(111) may be due to the variation of the lattice constants which increase from PdCu (3.81 Å) to PdAu (4.05 Å). It is noted that the adsorption configuration of acetylene on these alloy surfaces is similar to that on Pd(111) and the C atoms bind to the surface Pd atoms.

2. $CHCH_2$

The intermediate vinyl $CHCH_2$ always has larger adsorption energies than C_2H_2. The favorite adsorption site over M(111) (M=Pd, Cu, Ag, Au) is the 3-fold hollow

with the adsorption energies of −2.84 eV, −1.89 eV, −1.28 eV and −1.64 eV over Pd(111), Cu(111), Ag(111) and Au(111). Introduction of Pd into Cu, Ag and Au surfaces also enhances the substrate-adsorbate interaction, as evidenced by the decreased adsorption energies from −2.04 to −2.31 eV on PdM(111), compared to −1.28 to −1.89 eV on M(111). The adsorption energies for vinyl are lowered to −2.31 eV, −2.04 eV and −2.05 eV for PdCu(111), PdAg(111) and PdAu(111). Structurally the CH group in vinyl shifts from a bridging site on M(111) to an atop Pd site on PdM(111).

3. CH_2CH_2

Ethylene adsorbs most favorably in the di-σ adsorption mode over Pd(111). The adsorption energy is calculated to be −0.93 eV, which is consistent with previous study[1]. On the three coin metals the adsorption geometry of ethylene becomes π mode and the adsorption energies are −0.17 eV, −0.05 eV and −0.09 eV on the Cu, Ag and Au surfaces respectively. as on Pd(111), ethylene also exhibits the di-σ mode in which the two C atoms interact with the two adjacent bridging Pd atoms on the PdM(111) surfaces. The adsorption energies are 0.25 eV higher than −0.93 eV on Pd(111).

4. CH_2CH_3

Ethyl adsorbs on the all surfaces with its CH_2 group bound an atop metal atom. On M(111) the adsorption energies range from −0.77 eV on Ag(111) to −1.72eV on Pd(111). On the PdM(111), it prefers to adsorb atop Pd rather than atop M, and the adsorption energies are about −1.5eV.

5. CH_3CH_3

Ethane is a saturated hydrocarbon molecule and it binds to the substrate through weak van der Waals interactions only. The predicted adsorption energies of ethane over the seven surfaces are less than −0.15eV.

6. $CHCH_3$

Ethylidene preferentially sits at the bridge site on Pd(111) with an adsorption energy of −3.76 eV. On the (111) surfaces of Cu, Ag and Au, the binding energies of ethylidene are reduced to −2.64 eV, −1.77 eV and −2.41 eV, respectively. The

preferential site is also the bridge site on the coin metal M surfaces. On all the PdM(111), the binding energy of $CHCH_3$ increases by about 0.4 eV in going from the Pd(111) (−3.76 eV) to ~ −3.3eV on over the PdM(111). The favored sites are the bridge site formed by two Pd atoms.

7. CHx(X=0∼3)

In all the favorable adsorption sites, the atom C bonding to the surfaces fulfills sp^3 configuration. Thus, CH_3 sits at a top site favorably; CH_2 occupies a bridge site and CH prefers to adsorb at a 3-fold fcc hollow site. Atomic carbon prefers to adsorb on the 3-fold hollow site with strong binding to all surfaces. It is more strongly bound to Pd than to M. The calculated adsorption energy over Pd(111) is −6.93 eV, whereas the values are −4.82eV, −3.33eV and −4.51eV on Cu(111), Ag(111) and Au(111). On PdM(111) facets, atomic carbon adsorbs at the 3-fold hollow site consisting of two Pd atoms and one M atom. The calculated adsorption energies are −5.95 eV, −5.89 eV and −6.12eV on the (111) surfaces of PdCu, PdAg and PdAu, respectively, which are about 1.0 eV higher than that on Pd(111).

The adsorption energies depend on the coordination number of CHx species with the substrate. Hence, following the atomic carbon, the adsorption energies of CH is the second largest, and CH_3 has the smallest one. As expected, the CHx intermediates are more strongly bound to Pd than to M sites.

9. CCHx(X=1∼3)

All the intermediates CCHx (x=1∼3) prefer to adsorb at 3-fold fcc hollow site. The C-C bond axis of adsorbed CCH and CCH_3 is perpendicular to the surface, whereas that of CCH_2 tilts about 80 degrees to the surface with CH_2 weakly interacting with the nearest surface Pd atom.

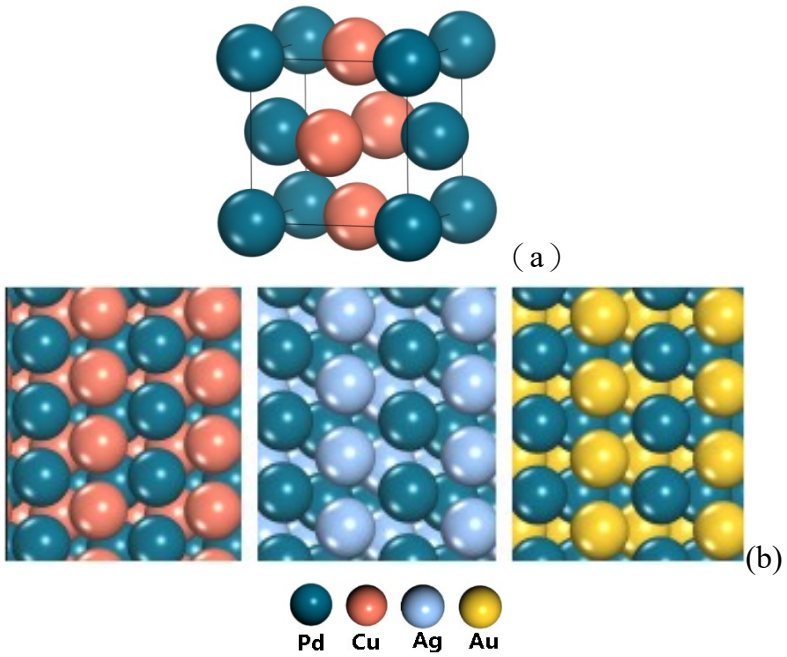

Figure S1 (a) FCC structures of PdM

(b) Top view structures for the (111) surfaces of PdCu, PdAg and PdAu.

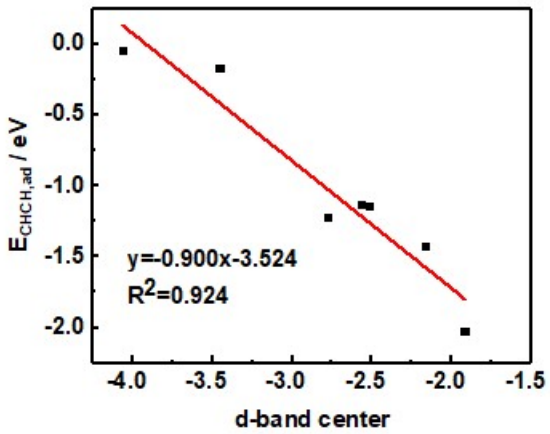

Figure S2 Relationship between CHCH adsorption energy and d-band center.

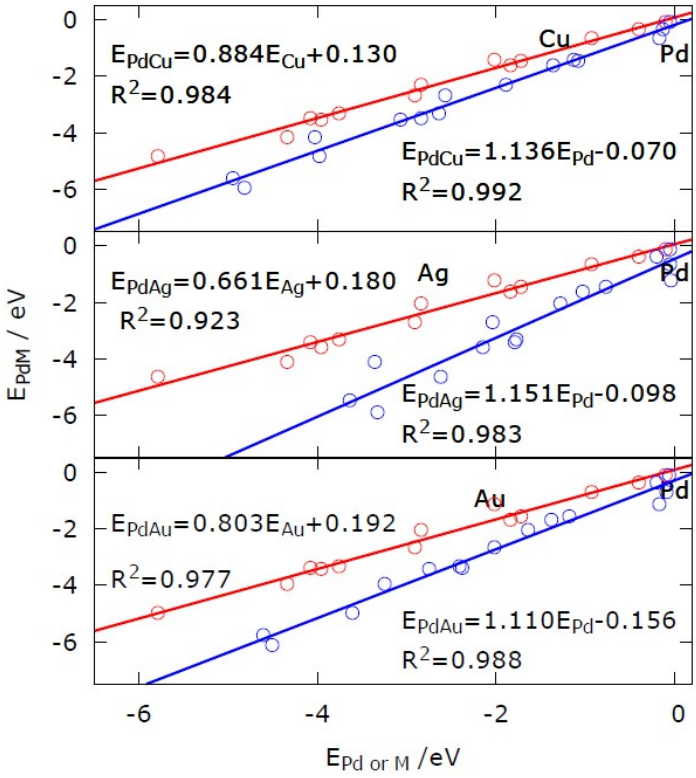

Figure S3 Adsorption energies of all species on PdM(111) plotted against that on Pd(111) and M(111) (M=Cu, Ag, Au).

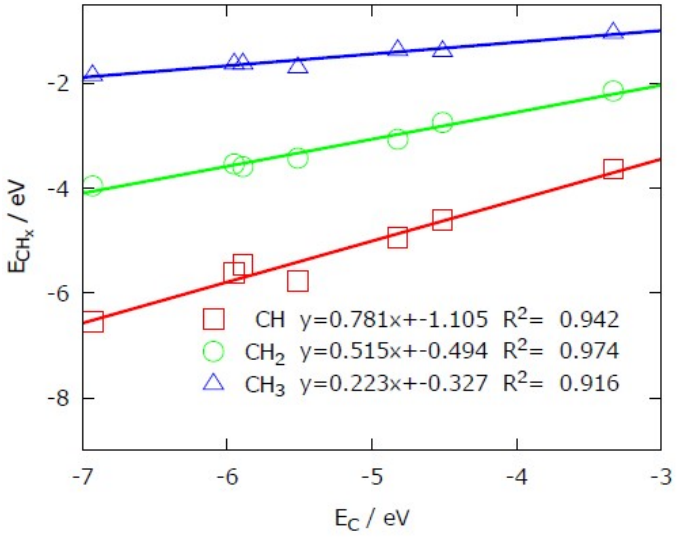

Figure S4 Adsorption energies of CH*x* intermediates (squares: *x*=1; circles: *x*=2; triangles: *x* =3) plotted against adsorption energies of atom C.

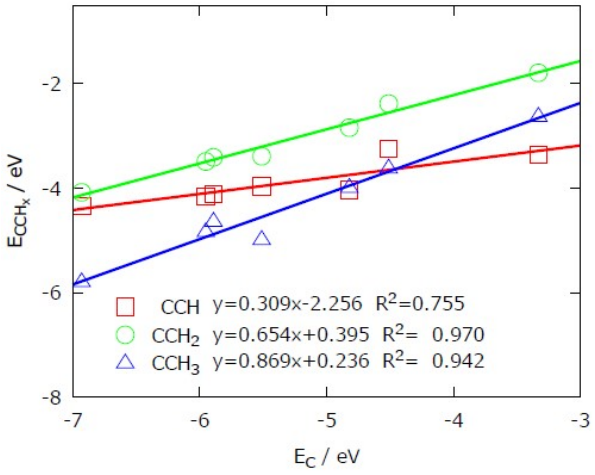

Figure S5 Adsorption energies of CCH*x* reactants plotted against adsorption energies of atom C.

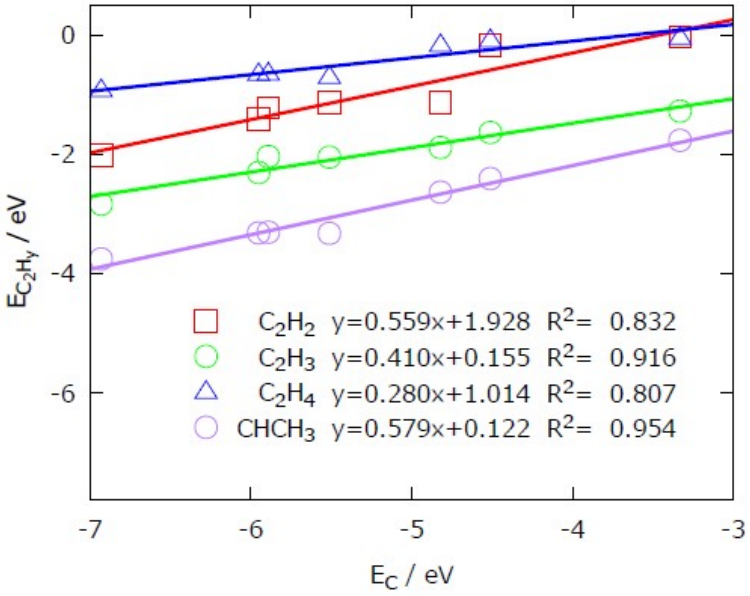

Figure S6 Adsorption energies of C_2H_y intermediates plotted against adsorption energies of atom C.

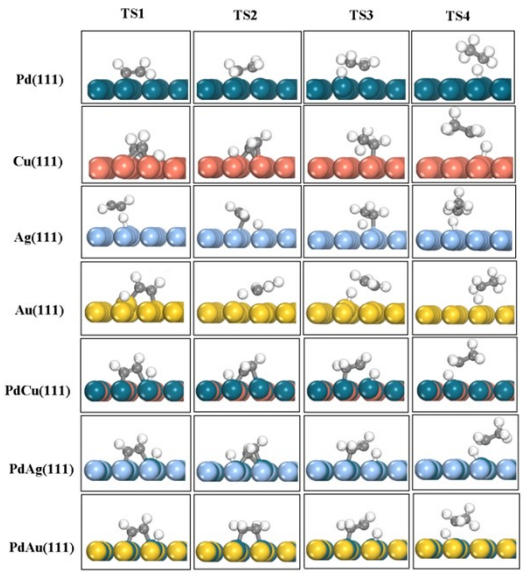

Figure S7 Transition states structures of CHCH hydrogenation to CH_3CH_3 over Pd(111), M(111) and PdM(11) (M=Cu, Ag, Au).

Table S1 Optimized structural parameters (pm) for the initial state (IS), transition state (TS), and final state (FS) of the CHCH→CH_3CH_3 reactions on Pd(111) and PdM(111) (M=Cu, Ag, Au) surfaces.

Pd(111)		parameter	IS	TS	FS
	CHCH→$CHCH_2$	C-C	137	139	145
		C-H	307	156	101
		C1-Pd	214,203,280	230,206,279	208,287,285
		C2-Pd	218,202,283	214,201,289	203,203
	$CHCH_2$→CH_2CH_2	C-C	145	145	144
		C-H	316	153	109
		C1-Pd	286,286,209	291,302,210	214,338,289
		C2-Pd	203,205,265	226,206,267	213,292,340
	CH_2CH_2→CH_2CH_3	C-C	140	145	151
		C-H	326	172	110
		C1-Pd	226,325,345	297,350,243	208,263,265
		C2-Pd	224,299,338	211,338,305	302,381,332
	CH_2CH_3→CH_3CH_3	C-C	1.50	1.51	1.52
		C-H	2.57	1.42	1.11
		C1-Pd	3.47,2.09,3.39	2.63,3.82,3.87	3.59,4.50,4.51
		C2-Pd	3.08,3.06,3.40	3.60,3.71,,4.22	3.89,4.45,4.35
Cu(111)	C_2H_2→$CHCH_2$	C-C	138	138	137
		C-H	333	161	111
		C1-Cu	205,208,211	201,211,217	199,215,228
		C2-Cu	204,210,210	231,221,229	236,298,325
	$CHCH_2$→CH_2CH_2	C-C	136	150	152
		C-H	300	133	110
		C1-Cu	232,334,332	297,260,302	333,302,358
		C2-Cu	238,311,314	209,322,324	203,343,342
	CH_2CH_2→CH_2CH_3	C-C	136	150	152
		C-H	300	133	111
		C1-Cu	232,334,368	260,297,371	333,302,395
		C2-Cu	238,311,314	209,324,352	203,349,352
	CH_2CH_3→CH_3CH_3	C-C	152	149	153
		C-H	279	186	110
		C1-Cu	305,331,428	375,397,399	468,421,435
		C2-Cu	208,296,356	293,398,398	420,455,455
Ag(111)	CHCH→$CHCH_2$	C-C	121	126	135
		C-H	374	144	109
		C1-Ag	436,422,467	328,347,366	308,343,322
		C2-Ag	434,426,462	345,355,406	237,227,347
	$CHCH_2$→CH_2CH_2	C-C	135	136	135

		C-H	294	153	109
		C1-Ag	220,255,333	232,295,377	280,364,410
		C2-Ag	327,330,321	300,342,350	278,368,376
	$CH_2CH_2 \rightarrow CH_2CH_3$	C-C	134	141	152
		C-H	356	152	111
		C1-Ag	312,391,402	295,341,348	317,367,397
		C2-Ag	314,393,387	258,382,384	222,395,396
	$CH_2CH_3 \rightarrow CH_3CH_3$	C-C	216	150	153
		C-H	300	165	110
		C1-Ag	226,341,350	302,406,410	425,514,514
		C2-Ag	324,367,431	380,415,392	425,518,519
Au(111)	$CHCH \rightarrow CHCH_2$	C-C	135	133	133
		C-H	322	177	109
		C1-Au	210,235,299	219,326,294	373,304,396
		C2-Au	300,250,209	305,209,325	382,207,384
	$CHCH_2 \rightarrow CH_2CH_2$	C-C	133	137	135
		C-H	382	160	109
		C1-Au	207,376,378	212,244,319	287,265,291
		C2-Au	305,396,371	294,278,285	284,275,395
	$CH_2CH_2 \rightarrow CH_2CH_3$	C-C	135	140	151
		C-H	427	175	110
		C1-Au	285,376,396	240,382,380	215,375,384
		C2-Au	289,398,360	304,380,333	311,386,287
	$CH_2CH_3 \rightarrow CH_3CH_3$	C-C	151	149	152
		C-H	368	166	110
		C1-Au	310,363,388	370,376,426	405,409,432
		C2-Au	215,383,376	290,4117,418	364,464,464
PdCu(111)	$CHCH \rightarrow CHCH_2$	C-C	134	134	133
		C-H	301	141	110
		C1-Pd(Cu)	205,214,276	199,278,243	200,326,326
		C2-Pd(Cu)	212,208,285	230,283,292	315,305,372
	$CHCH_2 \rightarrow CH_2CH_2$	C-C	138	139	142
		C-H	268	162	109
		C1-Pd(Cu)	205,216,335	206,235,326	219,291,334
		C2-Pd(Cu)	307,235,322	318,226,339	295,218,335
	$CH_2CH_2 \rightarrow CH_2CH_3$	C-C	142	145	151
		C-H	279	165	110
		C1-Pd(Cu)	222,296,334	240,296,347	325,303,389
		C2-Pd(Cu)	291,220,329	301,211,332	355,209,349
	$CH_2CH_3 \rightarrow CH_3CH_3$	C-C	151	150	152
		C-H	252	157	111
		C1-Pd(Cu)	307,298,399	361, 382, 437	428,418,472
		C2-Pd(Cu)	211,328,343	263,283,288	342,429,439

PdAg(111)	$CHCH \rightarrow CHCH_2$	C-C	132	132	134
		C-H	279	168	110
		C1-Pd(Ag)	277,202,260	278,198,282	338,200,314
		C2-Pd(Ag)	206,284,257	216,290,287	321,302,341
	$CHCH_2 \rightarrow CH_2CH_2$	C-C	139	139	143
		C-H	302	166	110
		C1-Pd(Ag)	204,216,327	206,233,333	217,293,337
		C2-Pd(Ag)	235,313,308	224,313,311	217,295,338
	$CH_2CH_2 \rightarrow CH_2CH_3$	C-C	142	150	151
		C-H	276	141	110
		C1-Pd(Ag)	218,292,337	208,303,337	208,363,350
		C2-Pd(Ag)	221,298,342	238,299,347	326,305,378
	$CH_2CH_3 \rightarrow CH_3CH_3$	C-C	151	150	153
		C-H	249	163	110
		C1-Pd(Ag)	301,306,395	378,355,369	318,434,483
		C2-Pd(Ag)	211,342,352	287,408,412	345,438,438
PdAu(111)	$CHCH \rightarrow CHCH_2$	C-C	130	132	133
		C-H	278	155	110
		C1-Pd(Au)	204,280,331	218,288,343	325,296,382
		C2-Pd(Au)	202,278,331	198,280,332	199,343,347
	$CHCH_2 \rightarrow CH_2CH_2$	C-C	138	139	143
		C-H	309	177	109
		C1-Pd(Au)	203,219,337	204,235,346	217,292,346
		C2-Pd(Au)	232,311,322	224,310,327	216,296,347
	$CH_2CH_2 \rightarrow CH_2CH_3$	C-C	142	147	151
		C-H	284	154	110
		C1-Pd(Au)	220,296,347	240,295,356	328,302,392
		C2-Pd(Au)	218,294,344	209,308,349	208,366,364
	$CH_2CH_3 \rightarrow CH_3CH_3$	C-C	150	150	152
		C-H	251	155	110
		C1-Pd(Au)	308,302,391	326,337,347	411,411,458
		C2-Pd(Au)	210,352,364	264,392,393	332,439,437

Table S2 The reaction energies (eV) of CHCH→CH_3CH_3 over Pd(111), M(111) and PdM(111) (M=Cu, Ag, Au) surfaces.

	Pd	Cu	Ag	Au	PdCu	PdAg	PdAu
CHCH+H→$CHCH_2$	0.17	−0.09	−0.83	−1.13	−0.01	0.07	−0.07
$CHCH_2$+H→CH_2CH_2	0.05	−0.67	−1.28	−1.17	−0.69	−0.60	−1.10
CH_2CH_2+H→CH_2CH	0.73	−0.07	−0.18	−0.55	0.19	0.21	0.13
CH_2CH_3+H→CH_3CH	−0.10	−1.15	−1.80	−1.24	−0.56	−0.64	−0.55

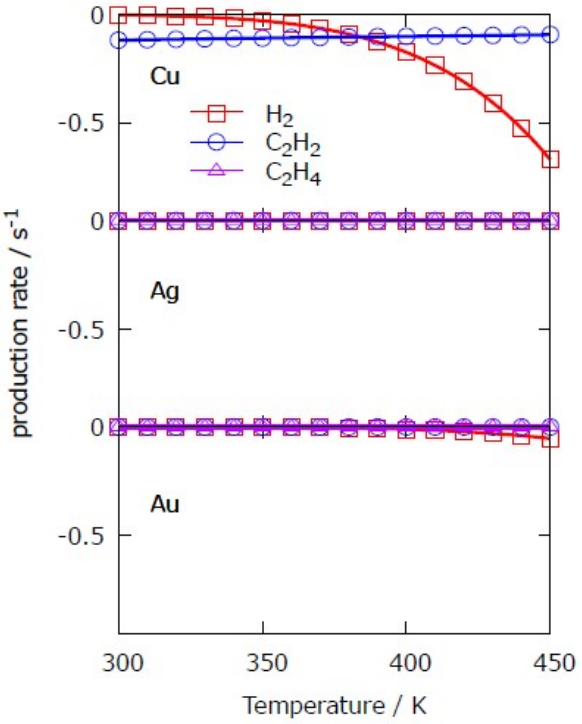

Figure S8 Reaction rates predicted by the microkinetic simulations of H_2, CHCH and CH_2CH_2 conversion over Cu(111), Ag(111) and Au(111) .

Table S3 Coverage of $CHCH_3$, CCH_3, CCH_2 and CCH at different temperature on Pd(111) and PdM(111).

Tempe-rature	Pd(111)						PdCu(111)						PdAg(111)						PdAu(111)					
	C	CH	CCH	CCH_2	CCH_3	$CHCH_3$	C	CH	CCH	CCH_2	CCH_3	$CHCH_3$	C	CH	CCH	CCH_2	CCH_3	$CHCH_3$	C	CH	CCH	CCH_2	CCH_3	$CHCH_3$
300	4.00E-05	2.27E-04	5.53E-04	4.92E-02	6.18E-03	4.49E-06	4.77E-16	7.15E-12	1.37E-11	5.61E-05	1.97E-04	3.59E-05	1.09E-19	1.74E-13	1.33E-06	1.20E-03	5.94E-04	1.20E-03	6.19E-15	3.10E-10	1.65E-05	2.15E-05	3.87E-05	2.12E-08
310	5.67E-05	2.84E-04	6.53E-04	6.58E-02	1.16E-02	8.46E-06	6.94E-16	1.10E-11	1.01E-11	4.25E-05	1.87E-04	3.90E-05	1.78E-19	3.10E-13	1.19E-06	1.07E-03	5.37E-04	1.08E-03	7.48E-15	3.29E-10	1.38E-05	1.80E-05	3.57E-05	3.28E-08
320	7.93E-05	3.50E-04	7.80E-04	7.00E-02	1.31E-02	1.32E-05	1.02E-15	1.66E-11	7.84E-12	3.16E-05	1.61E-04	3.74E-05	2.86E-19	5.41E-13	1.04E-06	8.87E-04	4.51E-04	8.96E-04	7.79E-15	3.17E-10	1.05E-05	1.38E-05	3.01E-05	4.53E-08
330	1.09E-04	4.25E-04	8.35E-04	6.61E-02	1.15E-02	1.19E-05	1.51E-15	2.47E-11	8.05E-12	2.67E-05	1.34E-04	3.38E-05	4.54E-19	9.27E-13	9.16E-07	7.10E-04	3.66E-04	7.19E-04	7.22E-15	2.78E-10	7.38E-06	9.80E-06	2.29E-05	5.48E-08
340	1.47E-04	5.09E-04	9.84E-04	6.15E-02	9.70E-03	1.06E-06	2.29E-15	3.63E-11	9.75E-12	2.46E-05	1.11E-04	3.01E-05	7.11E-19	1.56E-12	8.32E-07	5.66E-04	2.96E-04	5.74E-04	6.31E-15	2.30E-10	4.92E-06	6.59E-06	1.62E-05	5.87E-08
350	1.96E-04	6.00E-04	1.17E-03	5.69E-02	8.11E-03	9.64E-06	3.55E-15	5.27E-11	1.26E-11	2.36E-05	9.21E-05	2.66E-05	1.10E-18	2.57E-12	7.81E-07	4.56E-04	2.42E-04	4.62E-04	5.51E-15	1.87E-10	3.25E-06	4.39E-06	1.09E-05	5.74E-08
360	2.56E-04	6.95E-04	1.25E-03	5.24E-02	6.75E-03	8.93E-06	5.60E-15	7.54E-11	1.68E-11	2.28E-05	7.60E-05	2.33E-05	1.68E-18	4.16E-12	7.51E-07	3.71E-04	2.00E-04	3.76E-04	5.05E-15	1.55E-10	2.21E-06	3.01E-06	7.30E-05	5.27E-08
370	3.29E-04	7.93E-04	1.39E-03	4.83E-02	5.62E-03	9.29E-06	9.00E-15	1.07E-10	2.24E-11	2.21E-05	6.22E-05	2.02E-05	2.53E-18	6.63E-12	7.36E-07	3.05E-04	1.67E-04	3.09E-04	5.03E-15	1.35E-10	1.59E-06	2.18E-06	4.92E-05	4.64E-08
380	4.15E-04	8.89E-04	1.54E-03	4.48E-02	4.68E-03	8.55E-06	1.46E-14	1.49E-10	2.97E-11	2.14E-05	5.04E-05	1.72E-05	3.78E-18	1.04E-11	7.31E-07	2.53E-04	1.41E-04	2.56E-04	5.48E-15	1.25E-10	1.22E-06	1.67E-06	3.38E-05	3.95E-08
390	5.12E-04	9.79E-04	1.69E-03	4.45E-02	3.92E-03	8.04E-06	2.39E-14	2.05E-10	3.91E-11	2.05E-05	4.05E-05	1.45E-05	5.59E-18	1.60E-11	7.32E-07	2.11E-04	1.19E-04	2.13E-04	6.51E-15	1.22E-10	9.95E-07	1.36E-06	2.38E-05	3.29E-08
400	6.20E-04	1.06E-03	1.89E-03	4.11E-02	3.29E-03	7.61E-06	3.92E-14	2.81E-10	5.07E-11	1.95E-05	3.21E-05	1.20E-05	8.18E-18	2.43E-11	7.37E-07	1.77E-04	1.02E-04	1.78E-04	8.27E-15	1.24E-10	8.53E-07	1.16E-06	1.70E-05	2.70E-08
410	7.35E-04	1.12E-03	2.01E-03	3.76E-02	2.76E-03	8.09E-06	6.41E-14	3.80E-10	6.49E-11	1.83E-05	2.53E-05	9.82E-06	1.19E-17	3.65E-11	7.43E-07	1.49E-04	8.71E-05	1.50E-04	1.10E-14	1.31E-10	7.60E-07	1.03E-06	1.24E-05	2.19E-08
420	8.54E-04	1.17E-03	2.24E-03	3.49E-02	2.33E-03	1.58E-07	1.04E-13	5.09E-10	8.20E-11	1.70E-05	1.97E-05	7.93E-06	1.71E-17	5.39E-11	7.51E-07	1.26E-04	7.48E-05	1.26E-04	1.52E-14	1.41E-10	6.95E-07	9.38E-07	9.18E-06	1.76E-08
430	9.72E-04	1.20E-03	2.38E-03	3.29E-02	1.97E-03	8.52E-07	1.68E-13	6.76E-10	1.02E-10	1.57E-05	1.52E-05	6.33E-06	2.44E-17	7.87E-11	7.57E-07	1.06E-04	6.44E-05	1.06E-04	2.13E-14	1.55E-10	6.48E-07	8.67E-07	6.85E-06	1.41E-08
440	1.09E-03	1.20E-03	2.57E-03	2.98E-02	1.67E-03	2.06E-07	2.70E-13	8.90E-10	1.26E-10	1.44E-05	1.17E-05	5.00E-06	3.46E-17	1.14E-10	7.63E-07	8.96E-05	5.56E-05	8.90E-05	3.01E-14	1.70E-10	6.11E-07	8.11E-07	5.15E-06	1.12E-08
450	1.19E-03	1.19E-03	2.74E-03	2.76E-02	1.43E-03	7.74E-07	4.77E-13	7.15E-10	1.53E-10	1.32E-05	8.97E-06	3.92E-06	1.09E-17	1.74E-13	7.67E-07	7.59E-05	4.82E-05	7.50E-05	4.28E-14	1.89E-10	5.80E-07	7.64E-07	3.90E-06	8.93E-09

Table S4 Elementary reaction net rates (s^{-1}) over Pd(111) and PdM(111) at 450K.

	r(s-1)@Pd(111)	r(s-1)@PdCu(111)	r(s-1)@PdAg(111)	r(s-1)@PdAu(111)
H_2* +* ↔ 2H*	3.65E-01	2.32E-01	2.18E-01	1.42E-01
C* + H* ↔ CH* + *	3.54E-02	3.56E-11	2.07E-12	1.27E-10
CH* + H* ↔ CH_2* +*	2.64E-03	4.20E-09	3.00E-09	4.80E-07
CH_2* + H* ↔ CH_3* +*	2.53E-03	4.37E-09	7.24E-09	4.70E-07
CH_3* + H* ↔ CH_4* +*	2.59E-03	2.02E-04	1.46E-04	1.25E-04
CC* + H* ↔ CCH*+ *	0.00E+00	0.00E+00	0.00E+00	0.00E+00
CCH* + H* ↔ CCH_2*+ *	−4.74E-01	−1.81E-06	1.82E-02	−2.20E-04
CCH* +H*↔CHCH*+ *	4.39E-01	1.81E-06	−1.82E-02	2.20E-04
CCH_2*+H*↔ $CHCH_2$*+ *	−4.67E-01	1.42E-02	−1.26E-01	2.28E-04
CCH_2*+H*↔CCH_3*+ *	−7.73E-03	−1.42E-02	1.44E-01	−7.81E-06
CCH_3*+H*↔ $CHCH_3$*+ *	−7.73E-03	−1.42E-02	1.44E-01	−7.81E-06
$CHCH_2$*+H*↔$CHCH_3$*+*	2.22E-02	1.99E-02	9.36E-04	7.79E-06
$CHCH_3$*+H*↔CH_2CH_3*+*	1.20E-02	5.63E-03	1.45E-01	−1.83E-08
CHCH*+H* ↔ $CHCH_2$*+*	8.29E-01	2.27E-01	1.37E-01	1.41E-01
$CHCH_2$*+H*↔CH_2CH_2*+*	3.41E-01	2.21E-01	1.04E-02	1.41E-01
CH_2CH_2*+H*↔CH_2CH_3*+*	6.18E-04	−1.00E-04	−8.26E-02	−1.57E-03
CH_2CH_3*+H*↔CH_3CH_3*+*	1.26E-02	5.53E-03	6.27E-02	1.57E-03
CHCH* + * ↔ 2CH*	−3.80E-02	4.11E-10	1.68E-11	2.40E-07
CH_2CH_2* + * ↔ $2CH_2$*	−3.36E-09	3.44E-14	1.99E-13	−3.15E-09
CH_2CH_3* +*↔CH_2*+ CH_3*	−7.25E-06	1.06E-10	4.21E-09	−3.84E-09
CH_3CH_3* + * ↔ $2CH_3$*	−2.58E-10	−3.90E-09	−7.20E-09	−2.33E-07
$CHCH_3$* + * ↔ CH* +CH_3*	2.53E-03	3.28E-09	2.94E-09	−2.40E-13
CCH* + * ↔ C* +CH*	3.54E-02	5.68E-19	7.34E-15	−1.96E-12
CC* +* ↔ 2C*	−3.09E-03	5.68E-11	5.25E-12	4.84E-07
CCH_2* + * ↔ C* +CH_2*	3.56E-07	3.72E-14	5.67E-15	−1.33E-12
CCH_3* + * ↔ C* +CH_3*	5.67E-07	3.56E-11	2.05E-12	−1.27E-10

$CHCH_2$*+*↔CH*+CH_2*	1.02E-04	6.18E-11	2.20E-11	−8.47E-12

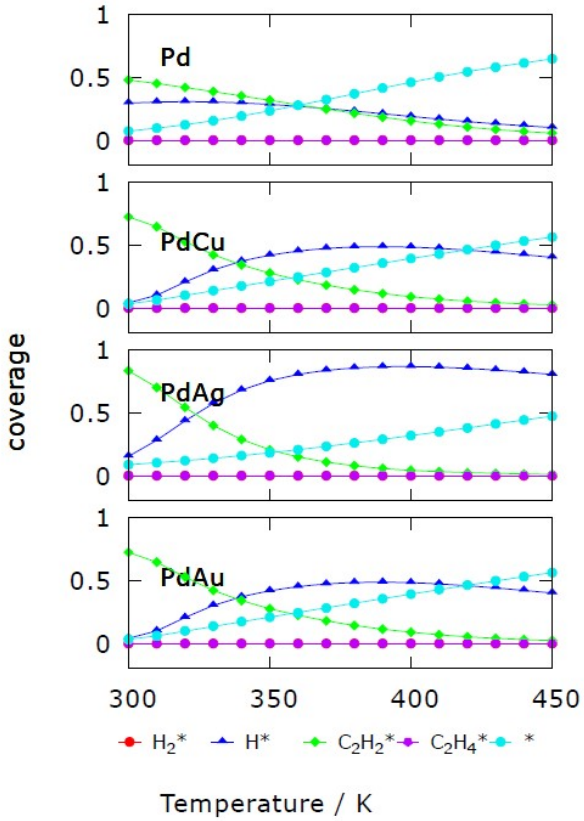

Figure S9 Coverage of main surface species for CHCH hydrogenation as a function of temperature.

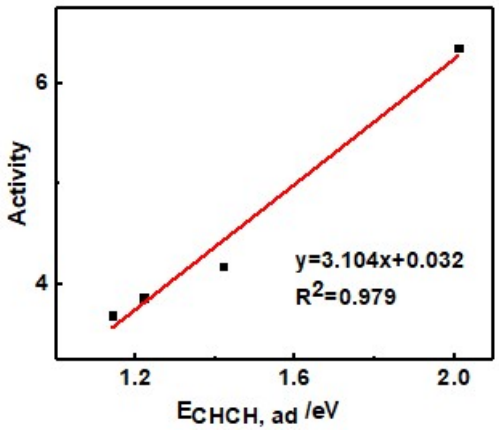

Figure S10 Relationship between activity measured by the consumption of CHCH and CHCH adsorption energy.

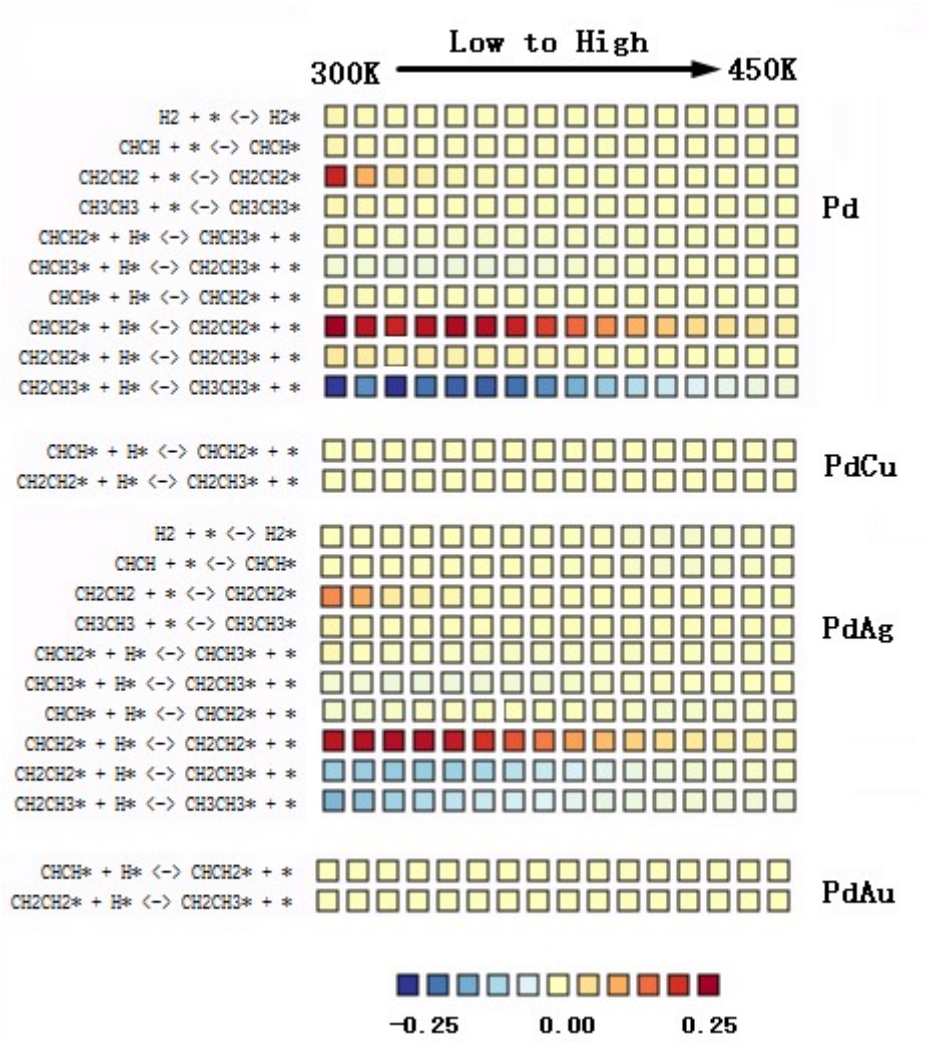

Figure S11 Degree of selectivity control of elementary step for CH_2CH_2 formation on Pd(111) and PdM(111) (M=Cu, Ag, Au) as a function of temperature.

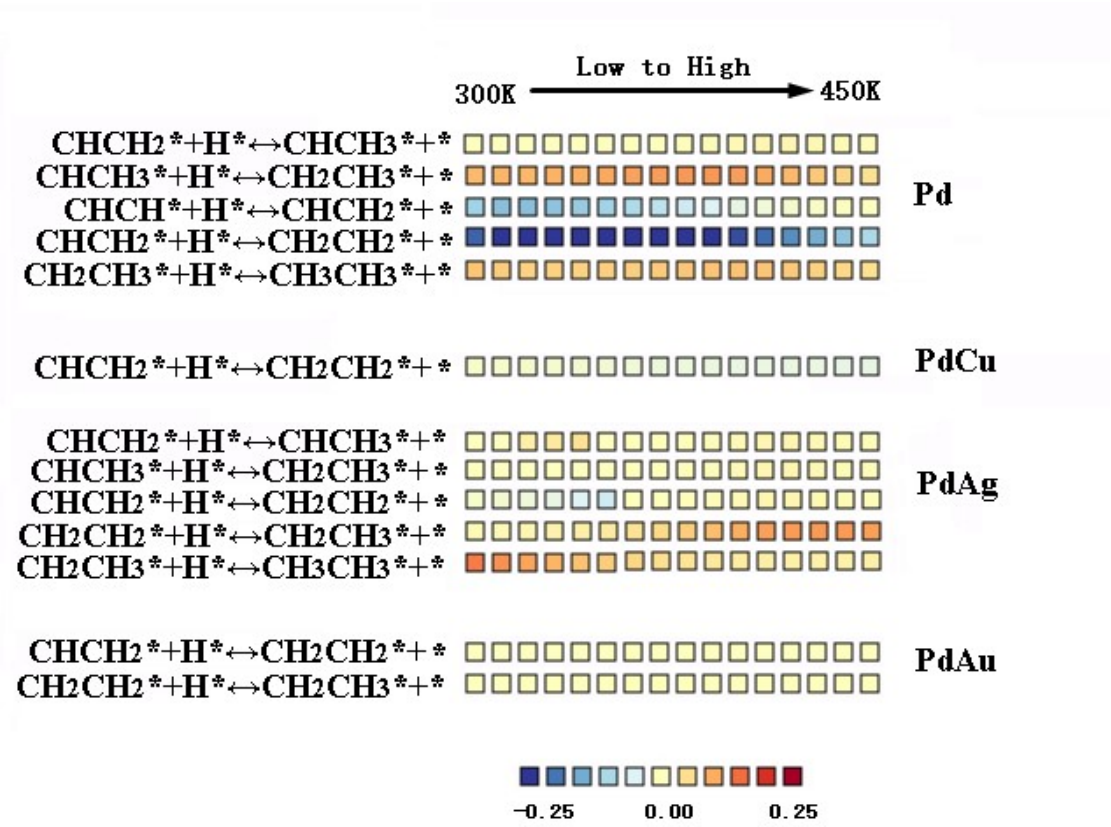

Figure S12 Degree of selectivity control of elementary step for CH_3CH_3 formation on Pd(111) and PdM(111) (M=Cu, Ag, Au) as a function of temperature.

Reference

(1) B.Yang, R.Burch, C.Hardacre, G. Headdock, P. Hu, *J. Catal.* 2013, **305**, 264–276.

(2) W. Liu, J. S. Lian, Q. Jiang, *Phys. Chem. C* 2007, **111**, 18189–18194.

(3) Y. Konishi, Y.Sainoo, K. Kanazawa, S. Yoshida, A. Taninaka, O. Takeuchi, H. Shigekawa, *Phys. Rev. B,* 2005, **71** 193410.